

ADH1C maintains the homeostasis of metabolic microenvironment to inhibit steatotic hepatocellular carcinoma

Kequan Xu^{a,b,1}, Tiangen Wu^{a,b,1}, Xiaomian Li^{a,b,1}, Xiao Zhang^{c,1}, Xinyu Liu^{a,b}, Shuxian Ma^{a,b}, Wenlong Dong^d, Jialing Yang^e, Yingyi Liu^{a,b}, Weixian Fang^{a,b}, Yi Ju^{a,b}, Yiran Chen^f, Caixia Dai^{a,b}, Zheng Gong^g, Wenzhi He^h, Zan Huang^h, Lei Chang^{a,b}, Weijie Ma^{a,b}, Peng Xia^{a,b,i,*}, Xi Chen^{a,b,**}, Yufeng Yuan^{a,b,j,**}

^a Department of Hepatobiliary & Pancreatic Surgery, Zhongnan Hospital of Wuhan University, Wuhan 430071, PR China

^b Clinical Medicine Research Center for Minimally Invasive Procedure of Hepatobiliary & Pancreatic Diseases of Hubei Province, Hubei, PR China

^c Department of Liver Surgery, West China Hospital of Sichuan University, No. 37, Guoxue Lane, Chengdu, Sichuan Province, PR China

^d University of Chinese Academy of Sciences, Beijing 100049, PR China

^e School of Basic Medical Sciences, Nanjing Medical University, Nanjing, Jiangsu Province, PR China

^f Liver Cancer Institute, Zhongshan Hospital, Key Laboratory of Carcinogenesis and Cancer Invasion, Ministry of Education, Fudan University, 180 Fenglin Road, Shanghai 200032, PR China

^g Department of Pharmacy, Union Hospital, Tongji Medical College, Huazhong University of Science and Technology, Wuhan 430022, PR China

^h College of Life Sciences, Hubei Key Laboratory of Cell Homeostasis, Wuhan University, Wuhan 430072, PR China

ⁱ Department of Chemistry, Department of Biochemistry and Molecular Biology, Institute for Biophysical Dynamics, The University of Chicago, Chicago, IL 60637, USA

^j TaiKang Center for Life and Medical Sciences, Wuhan University, Wuhan 430071, PR China

ARTICLE INFO

Keywords:

Hepatocellular carcinoma
ADH1C
PPARα
Fatty acid metabolism
Metabolic reprogramming

ABSTRACT

Steatotic hepatocellular carcinoma (HCC) has emerged as a significant subtype of HCC. Understanding the complex tumor microenvironment in HCC is particularly important for stratifying patients and improving treatment response. In this study, we performed proteomic analysis on clinical samples of steatotic HCC and identified human-specific gene alcohol dehydrogenase 1C (ADH1C) as a key factor. ADH1C is a favorable prognostic factor in both steatotic and non-steatotic HCC. ADH1C promotes fatty acid degradation through a novel non-enzymatic function, inhibiting the development of hepatocellular carcinoma. Specifically, *in vitro* experiments revealed that ADH1C interacts with splicing factor retinitis pigmentosa 9 (RP9) to enhance the splicing of key transcription factor peroxisome proliferator activated receptor alpha (PPARα) pre-mRNA, which is crucial for fatty acid degradation. The regulation of the ADH1C/RP9/PPARα axis was supported by *in vivo* experiments and clinical relevance. This leads to a reduction in the critical metabolite palmitic acid, subsequently decreasing the palmitoylation levels of oncogenic protein TEA domain transcription factor 1 (TEAD1), thereby regulating the hippo pathway and subsequent cell proliferation inhibition. Additionally, we found that ADH1C and PPARα can serve as combined biomarkers to distinguish between patients with steatotic and non-steatotic HCC. Combination therapy targeting ADH1C and anti-programmed cell death protein 1 (PD1) enhances the response of steatotic HCC to anti-PD1 immunotherapy. Our study revealed a central role of ADH1C/PPARα in lipid metabolism and HCC suppression. Targeting lipid metabolism via ADH1C/PPARα may provide new therapeutic strategies for the treatment of liver cancer.

* Corresponding author.

** Corresponding authors at: Department of Hepatobiliary & Pancreatic Surgery, Zhongnan Hospital of Wuhan University, Wuhan 430071, PR China.

E-mail addresses: surexkq@whu.edu.cn (K. Xu), wtg666@whu.edu.cn (T. Wu), lixiaomian@whu.edu.cn (X. Li), zhangxiao94@stu.scu.edu.cn (X. Zhang), 2020305232003@whu.edu.cn (X. Liu), 2018305231095@whu.edu.cn (S. Ma), dongwenlong16@mails.edu.cn (W. Dong), jlyang@stu.njmu.edu.cn (J. Yang), 2013302180342@whu.edu.cn (Y. Liu), 2019305232132@whu.edu.cn (W. Fang), 2021305233137@whu.edu.cn (Y. Ju), 23111210121@m.fudan.edu.cn (Y. Chen), caixiadai22@whu.edu.cn (C. Dai), 2022XH5004@hust.edu.cn (Z. Gong), hewz@whu.edu.cn (W. He), z-huang@whu.edu.cn (Z. Huang), reniorchang@whu.edu.cn (L. Chang), mawj1990@whu.edu.cn (W. Ma), pengxia@uchicago.edu (P. Xia), chenxi2022@whu.edu.cn (X. Chen), yuanyf1971@whu.edu.cn (Y. Yuan).

¹ These authors contributed equally to this work.

<https://doi.org/10.1016/j.metabol.2025.156267>

Received 31 October 2024; Accepted 11 April 2025

Available online 13 April 2025

0026-0495/© 2025 Elsevier Inc. All rights are reserved, including those for text and data mining, AI training, and similar technologies.

1. Introduction

Hepatocellular carcinoma (HCC) is one of the most prevalent and deadly cancers worldwide [1]. With the prevalence of antiviral drugs for hepatitis B and the current population's high-fat, high-sugar dietary habits, the main type of HCC has gradually shifted from Hepatitis B virus (HBV)-related HCC to non-viral HCC (approximately 38 % being steatotic HCC) [2]. The tumor microenvironment of steatotic HCC is more complex compared to traditional HCC, particularly due to the metabolic reprogramming associated with steatotic HCC, which influences tumor progression and immune response [3,4]. Research by Mathias Heikenwalder et al. has demonstrated that anti-PD-1 therapy has limited efficacy in treating steatotic HCC and might even facilitate disease progression [4]. Currently, there are no targeted drugs available specifically for steatotic HCC. Therefore, it is imperative to elucidate the mechanisms underlying the occurrence and development of steatotic HCC, as well as its association with metabolic reprogramming, to identify effective therapeutic targets.

Normal hepatocytes primarily generate ATP through fatty acid oxidation (FAO) and oxidative phosphorylation (OXPHOS), utilizing fatty acids as their main energy substrate. The liver maintains energy homeostasis through fatty acid catabolism while simultaneously synthesizing lipoproteins and phospholipids to support physiological functions [5]. In contrast, HCC cells exhibit significant metabolic reprogramming characterized by enhanced de novo fatty acid synthesis and suppressed catabolic processes (via FAO downregulation) to sustain rapid proliferation [5]. However, it remains experimentally unverified whether this FAO downregulation pattern persists in metabolically hyperactive steatotic HCC cells, or what specific role FAO might play in steatotic HCC pathogenesis.

In this study, we performed proteomic analysis of steatotic HCC and identified a human-specific gene, alcohol dehydrogenase 1C (*ADH1C*), as a key factor. Alcohol dehydrogenase (ADH) class I isozymes are considered the major contributors to ethanol metabolism in all species [6]. *ADH1C* is a member of the alcohol dehydrogenase family responsible for the breakdown of ethanol, retinol, other fatty alcohols, hydroxysteroids, and lipid peroxidation products in other cancers [7,8]. However, human-specific *ADH1C* may have additional complex functions in the human system [9,10]. The γ -subunit protein expressed by *ADH1C* is primarily expressed in the postnatal liver, which corresponds to the maturation time of the liver metabolic system [9,10]. Our research shows that *ADH1C* was closely associated with steatotic HCC and nonsteatotic HCC, and served as a favorable prognostic factor, even though none of these HCC patients have a history of alcohol abuse. *ADH1C* inhibits HCC by promoting FAO through a novel mechanism beyond enzyme activity.

2. Results

2.1. Clinical, pathological and molecular features of steatotic HCC

We analyzed clinical and pathological data from 25 steatotic HCC and 47 nonsteatotic HCC patients at Zhongnan Hospital of Wuhan University. Consistent with previous reports [2,11,12], Steatotic HCC displayed pronounced lipid accumulation, hepatocellular ballooning, inflammatory infiltration, and fibrosis, alongside enhanced proliferative capacity (Fig. 1A). Clinically, steatotic HCC correlated with higher inflammation and fibrosis grades and larger tumor size, whereas nonsteatotic HCC exhibited greater vascular invasion and malignancy (Table S4). Despite these differences, survival outcomes were comparable between the two groups (Fig. 1B), implying that steatotic HCC may influence survival through mechanisms other than tumor invasiveness and malignancy, warranting further exploration of its proliferative potential.

2.2. *ADH1C* was identified as a key regulatory factor in steatotic HCC

To investigate the distinct mechanisms of steatotic HCC, we conducted proteomic analysis on three pairs of steatotic and non-steatotic HCC tissues. GSEA, KEGG, and GO analyses highlighted the enrichment of metabolic and tumor-related pathways, including "Fatty acid degradation" and "PPAR signaling pathway," in steatotic HCC (Fig. S1A–B). Notably, *ADH1C*, a human-specific alcohol dehydrogenase, was the most significantly downregulated protein (Fig. 1C). Its suppression in steatotic HCC samples without alcohol abuse history suggests a potential non-enzymatic role, possibly pivotal in steatotic HCC pathogenesis.

Further analysis revealed that *ADH1C* is underexpressed in both steatotic and non-steatotic HCC compared to adjacent non-tumor tissues (Fig. S1C–D), with significantly lower levels in steatotic HCC (Fig. 1D–F). High *ADH1C* expression correlated with improved prognosis in both HCC subtypes (Fig. S1E–J). To investigate *ADH1C*'s role, we overexpressed *ADH1C* in low-expressing HCC-LM3 and Hep-G2 cells and knocked it down in high-expressing Huh-7 and MHCC-97H cells (Fig. S1K–O). *ADH1C* overexpression reduced triglycerides (TG) and free fatty acids (FFA), while knockdown increased them, suggesting its role in inhibiting steatotic HCC (Fig. 1G–H). *ADH1C* also suppressed HCC cell proliferation in clonogenic and CCK8 assays (Fig. 1I–K). To determine if these effects were enzyme-dependent, we created an enzymatically inactive *ADH1C* mutant (*ADH1C*-MUT), which similarly impacted lipid metabolism and proliferation, confirming a non-enzymatic mechanism (Fig. S1P–T). Notably, *ADH1C*'s anti-proliferative and fatty acid oxidation effects surpassed other ADH family members (Fig. S1V–W), further supporting its non-enzymatic function. In a myr-Akt/NRas12D-induced steatotic HCC mouse model, *ADH1C* overexpression reduced tumor burden, TG/FFA levels, lipid accumulation, and proliferation (Fig. 1L–S). These findings suggest *ADH1C* inhibits steatotic HCC progression, though its dependency on steatosis remains unclear.

2.3. *ADH1C* promotes fatty acid oxidation in HCC

To investigate altered lipid levels in HCC cells, integrated lipidomics and transcriptomics analyses revealed enrichment in the "Fatty acid degradation" pathway (Figs. S2A, S3), with PPARa potentially playing a pivotal role (Fig. S4) [13]. The accumulation of acylcarnitines, indicative of β -oxidative capacity [14,15], was linked to the downregulation of CPT2 [16], a critical gene for fatty acid oxidation, providing a plausible explanation for hepatic steatosis in HCC. Lipidomics analysis demonstrated that *ADH1C* knockdown increased intracellular acyl-carnitine accumulation, while its overexpression reduced acyl-carnitine levels and enhanced β -oxidation (Fig. S2B). Conversely, *ADH1C* downregulation impaired β -oxidation (Fig. S2C). Consistent with these findings, *ADH1C* overexpression upregulated fatty acid degradation genes at both mRNA and protein levels, whereas knockdown had the opposite effect (Fig. S2D–E), confirming *ADH1C*'s role in promoting fatty acid degradation in HCC cells.

2.4. PPARa is required for *ADH1C* functions in β -oxidation and cell proliferation in HCC

Multiple omics analyses and our experiment demonstrated that the suppressive role of *ADH1C* in HCC is tightly associated with β -oxidation. To verify whether β -oxidation is required for *ADH1C* tumor suppressor function in HCC, PPARa was knocked down in *ADH1C* overexpressing cells (Fig. S5). PPARa downregulation restored TG and FFA production and lipid accumulation in *ADH1C* overexpressing cells (Fig. S2F–H). Consistently, PPARa knockdown also offset the enhanced β -oxidation induced by *ADH1C* overexpression (Fig. S2I). Accordingly, PPARa knockdown reversed the upregulated expression of fatty acid β -oxidation-related genes *ADH1C* overexpression (Fig. S2J–K). In contrast,

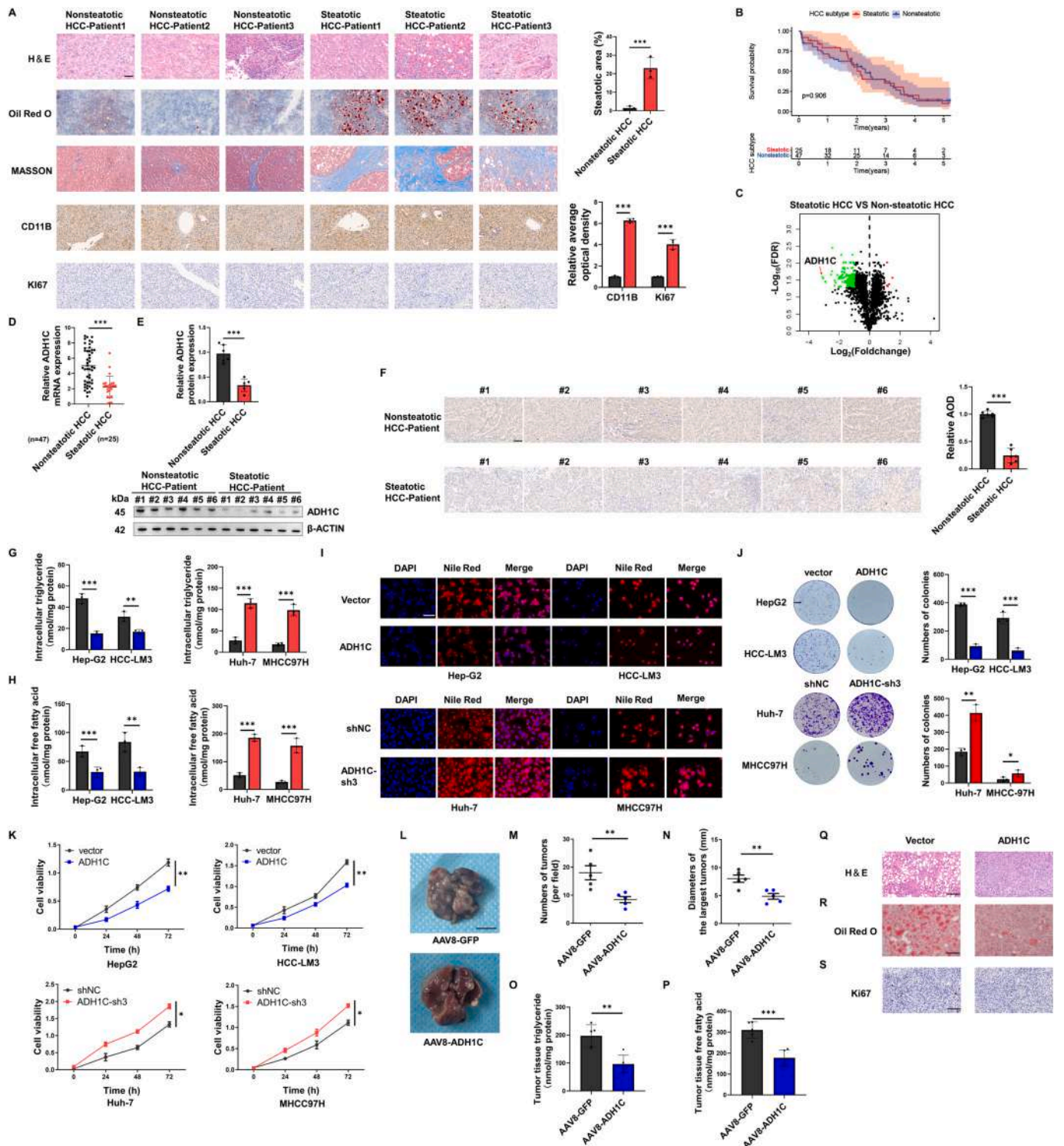


Fig. 1. ADH1C identified as a key regulatory factor in steatotic hepatocellular carcinoma (HCC).

A HE, Oil Red O, MASSON, CD11B and Ki67 staining in three tissues of steatotic HCC tissues and nonsteatotic HCC. Scale bars, 100 μ m. B Kaplan-Meier survival curve of patients with steatotic HCC and nonsteatotic HCC. C Volcano maps show differentially expressed proteins in the “fatty acid degradation” pathway. Green: $\log_2FC < -1$, $FDR < 0.05$; red: $\log_2FC > 1$, $FDR < 0.05$. D–E ADH1C mRNA levels and protein expression in steatotic HCC and nonsteatotic HCC tissues. F Immunohistochemistry shows the protein expression distribution of ADH1C in steatotic HCC and nonsteatotic HCC tissues. Scale bars, 100 μ m. G Intracellular triglyceride content in cells with overexpression or knockdown of ADH1C (biochemical method). H Overexpression or knockdown of ADH1C Intracellular free fatty acid content in cells (biochemical method). I Nile red staining shows neutral lipid content in ADH1C overexpressing or knockdown cells. Scale bars, 100 μ m. J Number of clones formed. Scale bars, 10 mm. K CCK8 method to detect the proliferation activity of ADH1C overexpression or knockdown cells. L Livers from myr-Akt/NRas12D infected mice with or without ADH1C overexpression. Scale bars, 10 mm. O–R Numbers of tumors (per field) (M), Diameters of the largest tumors(N), Tumor tissue triglyceride(O) and Tumor tissue free fatty acid(P) in livers from myr-Akt/NRas12D infected mice with or without ADH1C overexpression. S–U HE(Q), Oil Red O (R) and Ki67(S) staining in livers from myr-Akt/NRas12D infected mice with or without ADH1C overexpression. Scale bars, 100 μ m. * ($p < 0.05$), ** ($p < 0.01$), or *** ($p < 0.001$).

PPAR α overexpression compensated for all the effects of ADH1C knockdown on HCC cell β -oxidation, TG and FFA production, lipid accumulation, and gene expression (Fig. S2F–K).

Integrated omics analyses and experimental validation revealed that ADH1C's tumor-suppressive role in HCC is might mediated through β -oxidation. PPAR α knockdown (Fig. S5) in ADH1C-overexpressing cells reversed the reduction in TG, FFA, and lipid accumulation, attenuated β -oxidation enhancement, and downregulated fatty acid β -oxidation-related genes (Fig. S2F–K). Conversely, PPAR α overexpression counteracted the effects of ADH1C knockdown (Fig. S2F–K). Notably, PPAR α knockdown nullified ADH1C's impact on HCC cell proliferation (Fig. S6A–B), indicating that ADH1C suppresses HCC by promoting β -oxidation via PPAR α . To validate the ADH1C/PPAR α axis in HCC in vivo, we demonstrated that PPAR α knockdown (Fig. S6C) rescued the ADH1C-mediated suppression of HCC proliferation, TG and FFA production, lipid accumulation, and fatty acid degradation gene expression in the liver (Fig. S6D–L). Furthermore, Complete PPAR α knockout abolished the effects of ADH1C modulation on HCC cell proliferation (Fig. S6M–N). These findings confirm that ADH1C inhibits HCC by promoting β -oxidation via PPAR α both in vitro and in vivo, suggesting that ADH1C initially suppresses steatotic HCC development, thereby impeding HCC progression.

2.5. ADH1C promotes phosphorylation of RP9 and enhances Intron 8–9 excision of PPAR α pre-mRNA

We have demonstrated the critical role of the ADH1C/PPAR α axis in steatotic HCC development and progression. To elucidate how ADH1C regulates PPAR α mRNA expression, we investigated whether ADH1C influences PPAR α alternative splicing, as ADH1C is not a transcription factor and did not affect PPAR α mRNA stability (Fig. 2A). Given that PPAR α is regulated by alternative splicing in the liver [17] and that ADH1C downregulation enhances PPAR α intron retention events (Fig. S7A), we hypothesized that ADH1C modulates PPAR α splicing. Using semi-quantitative PCR with intron-spanning primers, we found that ADH1C overexpression promoted the excision of intron 8 between PPAR α exons 8–9, increasing the expression of spliced mRNA while decreasing unspliced mRNA levels. Conversely, ADH1C downregulation had the opposite effect (Figs. 2B, S7C, D). No significant changes were observed in other intron regions, including intron 4–5 and intron 7–8, suggesting that ADH1C specifically targets intron 8. To identify proteins involved in this process, we performed ADH1C IP followed by LC-MS/MS and RNA pull-down assays targeting PPAR α mRNA. Four proteins commonly overlapped in ADH1C-interacting proteins and PPAR α mRNA-interacting proteins (Fig. 2C), of which RP9 is a splicing factor that regulates pre-mRNA splicing and the functions of other proteins are mRNA translation and protein post-translational modification. Furthermore, we found that ADH1C did not affect the translation process of PPAR α (Fig. 2D). Co-IP experiments confirmed the interaction between ADH1C and RP9 (Fig. 2E, F). Further RNA pull-down assays using in vitro transcribed PPAR α mRNA fragments revealed that RP9 specifically binds to PPAR α exon 8 (Figs. 2G, H, S7G, H). ADH1C overexpression enhanced the binding of RP9 to PPAR α exon 8, while ADH1C knockdown reduced it (Fig. 2I). We also constructed a PPAR α -MUT with a deleted RP9-binding site (ACGCUGGUGGCCAAGCUGGUGGC-CAAUGGCAUCCAGAACAAGGAGGCGGAGGUCCGCA) predicted by catRAPID, RPISeq, and RNAinter. The PPAR α -WT, but not PPAR α -MUT, mRNA bound to RP9 (Fig. 2J). Given that intron 8–9 retention would lead to abnormal PPAR α translation, we overexpressed the PPAR α variant in HCC cells but observed no effects on cell proliferation or lipid content (Fig. S8). This suggests that ADH1C downregulation may produce a loss-of-function PPAR α variant lacking the ligand-binding domain encoded by exon 9 [18–20]. Collectively, our results indicate that ADH1C enhances PPAR α pre-mRNA splicing through RP9, increasing mature PPAR α mRNA levels and exerting its inhibitory effects on HCC.

The mechanism by which ADH1C exerts splicing regulatory functions through RP9 is not yet clear, but based on existing research, the post-translational modification of RP9's protein translation may be a key regulatory factor for its splicing activity [21]. The PhosphoSitePlus website [22] indicates that RP9 has several ubiquitination, acetylation, and phosphorylation sites (Fig. S9A). Further experimental validation revealed that overexpression or knockdown of ADH1C does not affect the protein ubiquitination and acetylation levels of RP9, but it was found that ADH1C increases the overall phosphorylation level of RP9, while knocking down ADH1C leads to the opposite result (Figs. 2K, S9B–C). Analysis of phosphoprotein enrichment by mass spectrometry showed that S169 is the only phosphorylation site of RP9 (Fig. 2L). Specific phosphorylation antibodies for RP9-S169 were generated and used for Western blotting, confirming that ADH1C indeed increases the phosphorylation of RP9 at S169, whereas knocking down ADH1C elicits the opposite effect (Fig. 2M). The phosphorylated RP9 is localized at nuclear speckles (rich in splicing factors and spliceosomes), where it functions in pre-mRNA splicing, while dephosphorylated RP9 is localized in the nucleoplasm [21]. Immunofluorescence analysis showed that RP9 is scattered in nuclear speckles and nucleoplasm, and overexpression of ADH1C increases the nuclear speckle localization of RP9, while knocking down ADH1C increases its nuclear matrix localization (Fig. 2N). We also designed a plasmid with a mutated phosphorylation site for RP9 (S169A), and the results showed that RP9-WT enhanced PPAR α pre-mRNA splicing, whereas RP9-MUT did not (Figs. 2O, S9D). This demonstrates that the splicing regulation of PPAR α by ADH1C/RP9 depends on the phosphorylation of RP9 at the S169 site. We also constructed an HCC cell line with stable RP9 knockout and found that in the absence of RP9, neither the overexpression nor knockdown of ADH1C resulted in changes in PPAR α splicing, lipid metabolism, or cell proliferation (Fig. S10). This demonstrates that the ADH1C-dependent splicing regulation of PPAR α by RP9 affects the overall phenotypic changes of HCC.

2.6. ADH1C competitively binds to RP9 and inhibits the dephosphorylation of RP9 by PPP1CA

ADH1C, neither a phosphokinase nor a phosphatase, cannot directly regulate RP9 phosphorylation. To identify intermediate proteins, co-IP-MS was performed, revealing 7 phosphatases and 17 kinases associated with RP9, including PPP1CA, a phosphatase [23–25] linked to splice abnormalities in various diseases (Table S5, Fig. 3A). Co-IP experiments validated the interaction between PPP1CA and RP9 (Fig. 3B–C), with PPP1CA overexpression reducing RP9 phosphorylation and downregulation increasing it (Fig. 3D). PPP1CA also regulated PPAR α intron 8–9 excision, opposing ADH1C's effect (Fig. 3E–F). ADH1C did not affect PPP1CA expression or phosphorylation (Fig. 3G). Immunofluorescence showed colocalization of ADH1C, PPP1CA, and RP9 in nuclear speckles (Fig. 3H). Truncated RP9 mutants revealed that the N-terminal region, rich in basic and acidic residues, is crucial for ADH1C-RP9 binding, while the C-terminal coil and zinc finger domains are not (Fig. 3I–J). PPP1CA exhibited a similar binding pattern to RP9 as ADH1C (Fig. 3K). Overexpression of ADH1C or PPP1CA reduced their respective interactions with RP9, while knockdown had the opposite effect (Fig. 3L). These results suggest that ADH1C competes with PPP1CA for RP9 binding, inhibiting PPP1CA-mediated RP9 dephosphorylation and regulating PPAR α pre-mRNA splicing.

2.7. ADH1C regulates HCC proliferation through Hippo signaling pathway

To understand how ADH1C regulates HCC progression, RNA-seq-based KEGG analysis identified the Hippo signaling pathway, which is influenced by the metabolic microenvironment [26,27], as a key pathway (Figs. 4A–B, S3A–D). The Hippo pathway primarily affects tumor cell proliferation by regulating the cell cycle and apoptosis.

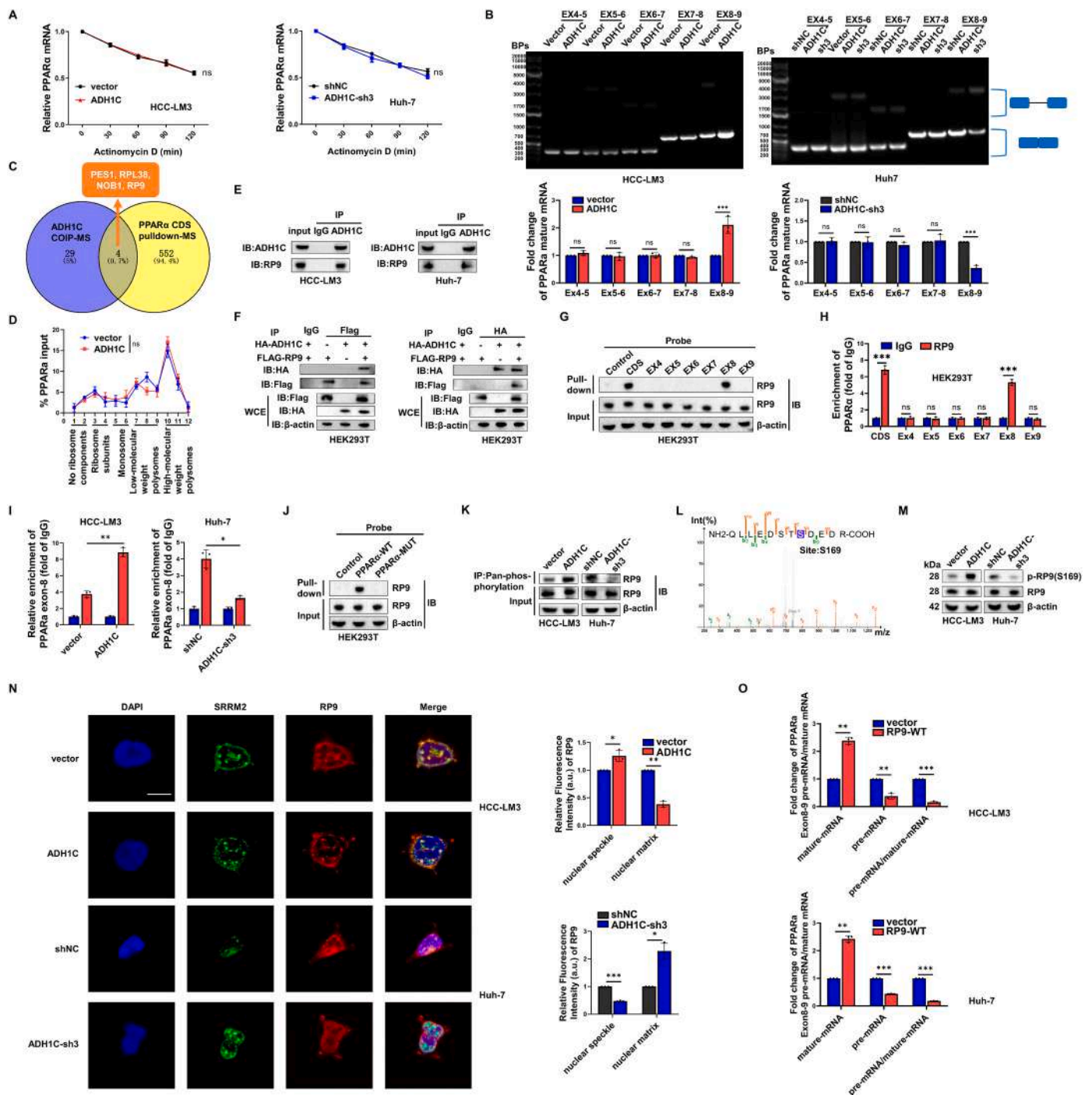


Fig. 2. ADH1C enhances the phosphorylation level of RP9 to exert its splicing function on PPARα pre-mRNA. A After treatment with actinomycin D (10 μg/ml), the mRNA level of PPARα was measured using qRT-PCR in ADH1C-overexpressing or -knockdown HCC cells. B Semi-quantitative PCR was used to measure the levels of intron-exclusive and intron-inclusive PPARα mRNA in ADH1C-overexpressing or -knockdown HCC cells. C Venn diagram showing four proteins that interact with both ADH1C protein and the PPARα CDS. D The polysomes of HCC-LM3 cells were extracted and subjected to a 10 % to 50 % sucrose gradient ultracentrifugation. The mRNA expression level in each fraction was determined by qRT-PCR. E Endogenous co-immunoprecipitation (co-IP) analysis demonstrating the specific binding of ADH1C and RP9. F Exogenous co-IP analysis validating the specific binding of ADH1C and RP9. G RNA pull-down analysis revealing the binding of full-length or truncated mRNA of PPARα CDS to RP9. H RNA immunoprecipitation followed by PCR analysis showing the enrichment of full-length or each truncated mRNA of PPARα CDS on RP9 co-immunoprecipitated complexes. I RIP-PCR analysis revealing that ADH1C enhances RP9 binding to PPARα Exon 8. J Deletion of the RP9-binding site abolished the interaction of RP9 with PPARα mRNA. K After protein phosphorylation enrichment, protein immunoblot analysis was performed to detect the phosphorylation level of RP9. L Mass spectrometry phosphoproteomic analysis revealed the specific phosphorylation sites of RP9 in HCC cells. M Protein immunoblot analysis was used to assess the phosphorylation level of specific phosphorylation sites of RP9. N Immunofluorescence analysis of the impact of ADH1C overexpression or knockdown on the subcellular localization of RP9, using SRRM2 antibody for nuclear speckle localization. Scale bars, 100 μm. O Semi-quantitative PCR analysis of the effect of RP9-WT on PPARα pre-mRNA splicing. * ($p < 0.05$), ** ($p < 0.01$), or *** ($p < 0.001$).

ADH1C overexpression altered the expression of Hippo pathway target genes, suppressing cell proliferation-related genes [26,27] (CTGF, GLI2, CCND1, CCNA2) and the anti-apoptotic gene SOX2, while enhancing the expression of the apoptotic gene AXIN1 (Fig. 4B). Conversely, ADH1C knockdown had the opposite effects. EDU assays and flow cytometry showed that ADH1C inhibited the G0/G1 to S phase transition in HCC cells, reducing the S phase population, while its knockdown promoted

cell cycle progression (Fig. 4C–D). Additionally, ADH1C increased apoptosis in HCC cells (Fig. 4E).

The canonical Hippo signaling pathway regulates the nuclear localization of the core gene YAP through phosphorylation cascades, thereby controlling downstream target genes [26,27]. However, ADH1C did not affect YAP levels or phosphorylation (Fig. 4F), suggesting a non-classical regulation of the Hippo pathway by ADH1C. Since YAP lacks

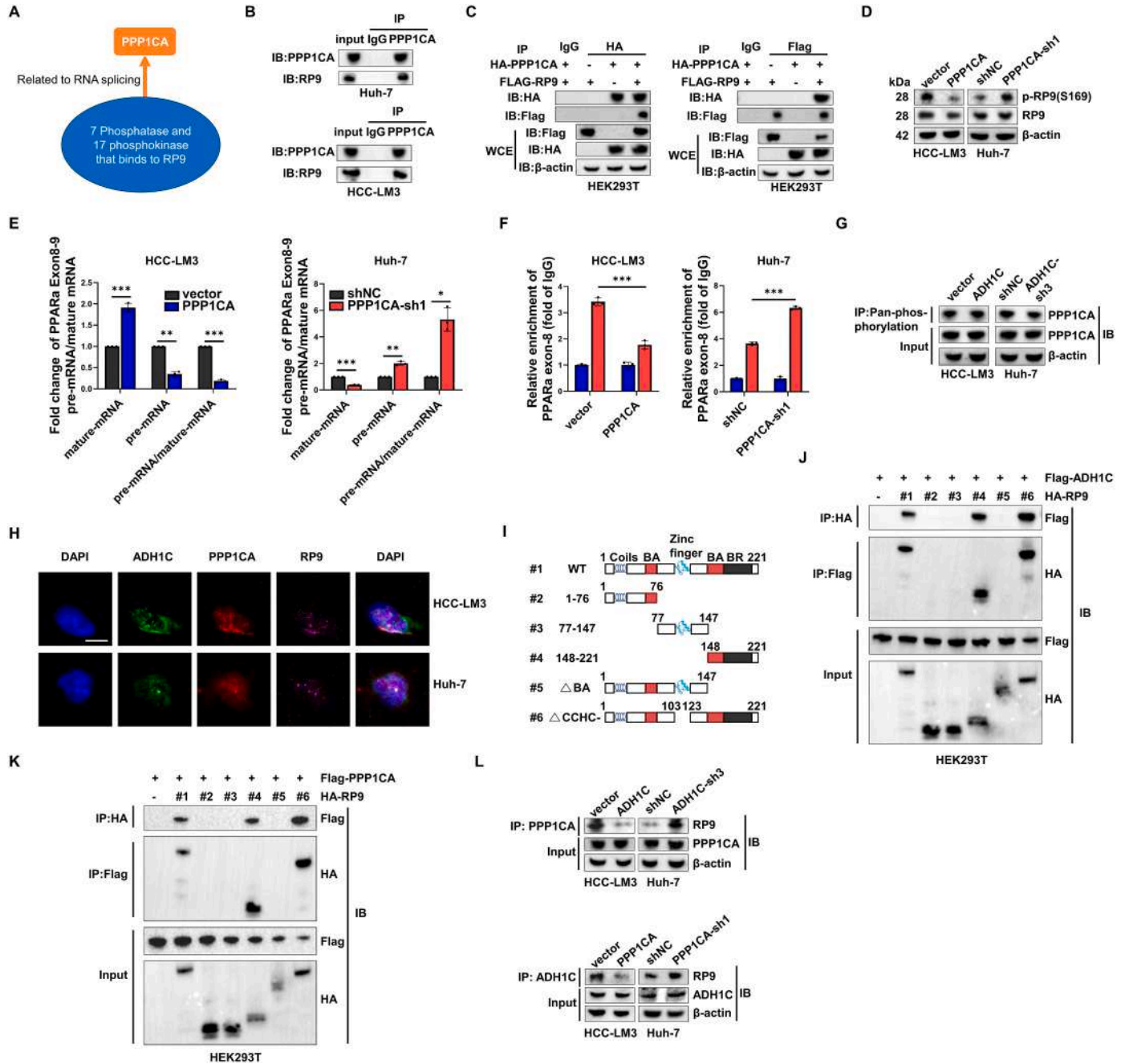


Fig. 3. ADH1C competitively binds to PPP1CA to regulate the phosphorylation level of RP9.

A Venn diagram depicting the RNA splice-associated proteins that interact with RP9, including kinases and phosphatases. B Endogenous co-immunoprecipitation (co-IP) analysis demonstrating the specific binding of RP9 and PPP1CA. C Exogenous co-IP analysis validating the specific binding of RP9 and PPP1CA. D After intervening in the expression of PPP1CA, the levels of RP9 and its phosphorylation were detected. E Semi-quantitative PCR analysis examining the effect of PPP1CA on PPARα pre-mRNA splicing. F RIP-PCR analysis revealing that PPP1CA inhibits RP9 binding to PPARα Exon 8. G After enrichment of phosphorylated proteins, protein immunoblot analysis was conducted to determine the effect of ADH1C on the protein level and phosphorylation status of PPP1CA. H Immunofluorescence analysis demonstrating the co-localization of ADH1C, RP9, and PPP1CA. I Schematic diagram illustrating the construction of full-length and truncated plasmids of RP9. J Co-IP analysis illustrating the binding of ADH1C and RP9 full-length or truncated domains. K Co-IP analysis demonstrating the binding of PPP1CA and RP9 full-length or truncated domains. L Co-IP analysis showing the impact of ADH1C or PPP1CA on their interaction with each other and RP9. * (p < 0.05), ** (p < 0.01), or *** (p < 0.001).

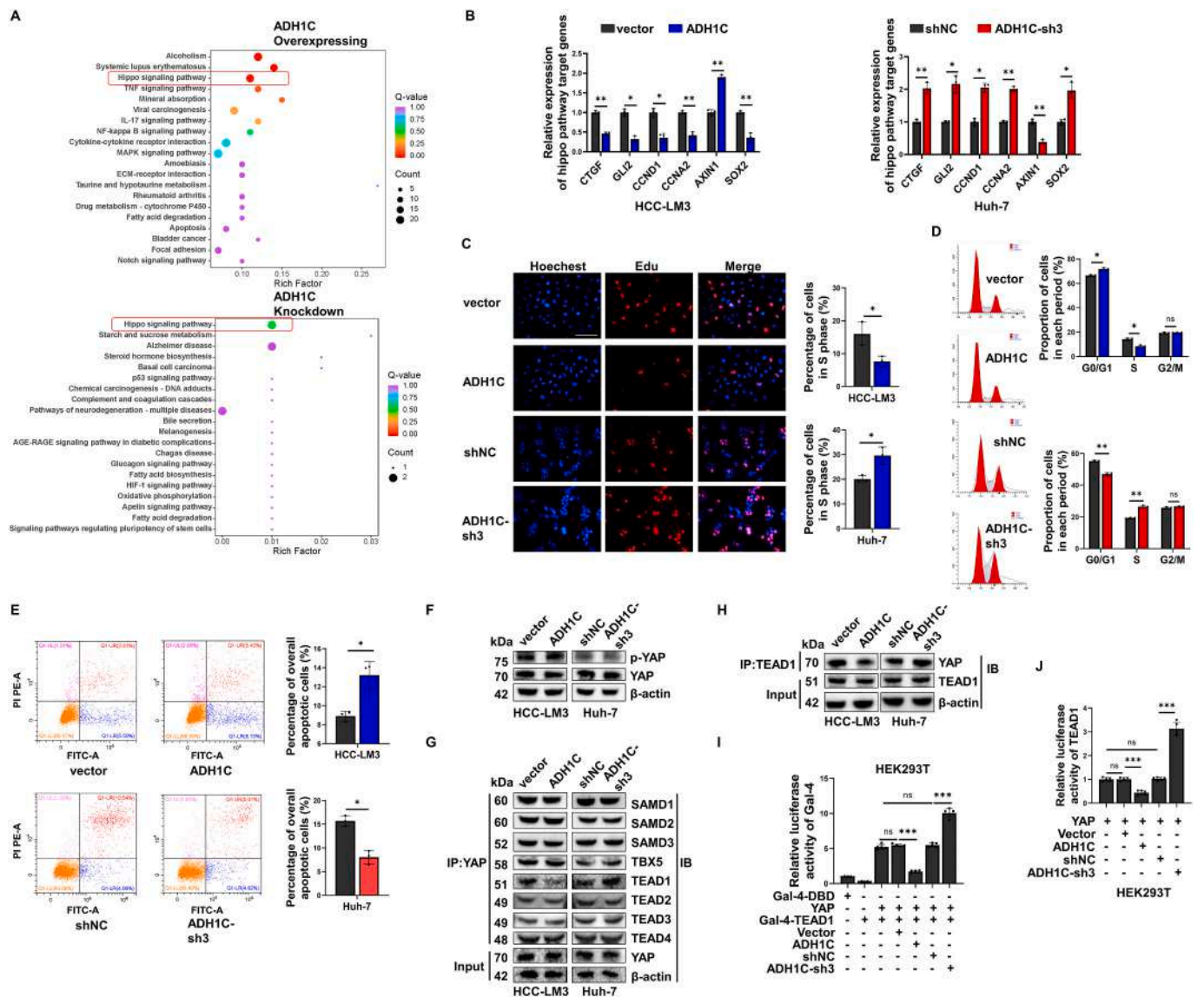


Fig. 4. ADH1C regulates the Hippo signaling pathway to inhibit HCC proliferation. A KEGG analysis was performed to identify differentially expressed genes in HCC cells with ADH1C overexpression or knockdown at the transcriptomic level. B mRNA levels of Hippo signaling pathway target genes in HCC cells with ADH1C overexpression or knockdown. C EDU staining marked proliferating active cells in HCC cells. Scale bars, 100 μ m. D Flow cytometry was used to screen HCC cells at different cell cycle phases and calculate their proportions. E Flow cytometry was used to screen HCC cells at different apoptosis stages and calculate their proportions. F Immunoblot analysis of YAP and its phosphorylated forms. G COIP was employed to pull down YAP protein and detect its binding ability with Hippo signaling pathway-related transcription factors. H COIP was employed to pull down TEAD1 protein and detect its binding ability with YAP. I Gal4 luciferase assay was conducted to evaluate the impact of ADH1C overexpression or knockdown on Gal4 luciferase activity, indicating changes in TEAD1-YAP binding capacity. J Luciferase reporter gene assay using TEAD1 was performed to assess the effect of ADH1C overexpression or knockdown on TEAD1 transcriptional activity. * ($p < 0.05$), ** ($p < 0.01$), or *** ($p < 0.001$).

a DNA-binding domain, it must form complexes with transcription factors to activate downstream gene transcription [28,29]. We found that ADH1C reduced the binding between TEAD1 and YAP, with the opposite effect observed upon ADH1C knockdown (Fig. 4G–H). In contrast, YAP binding to other transcription factors was unaffected by ADH1C overexpression or knockdown (Fig. 4G). Using a galactose-responsive GAL4 luciferase reporter, we showed that ADH1C knockdown activated GAL4-responsive luciferase in the presence of YAP [29], indicating enhanced TEAD1-YAP transcriptional activity, while ADH1C overexpression had the opposite effect (Fig. 4I). Consistently, ADH1C reduced TEAD1 reporter gene activity, indicating inhibition of its transcriptional function,

with the opposite effect upon ADH1C knockdown (Fig. 4J). Thus, ADH1C inhibits the TEAD1-YAP interaction, thereby suppressing HCC cell proliferation.

2.8. ADH1C regulates palmitic acid concentration to inhibit palmitoylation of TEAD1 and formation of TEAD1-YAP complex

TEAD1 is regulated by lipid metabolism and influences the TEAD1-YAP complex formation [29]. Reanalysis of lipidomics in HCC cells with ADH1C overexpression or knockdown revealed that ADH1C downregulated all lipid metabolite levels, with the most significant

changes in TGs, phosphatidylcholines (PC), phosphatidylinositols (PI), and FFA (Fig. 5A). Among these, palmitic acid (PA), which positively regulates TEAD1 palmitoylation and TEAD1-YAP complex formation [38], showed the highest fold change (Figs. 5B–C, S3E–J). Biochemical assays confirmed that ADH1C negatively regulated PA levels in HCC cells (Fig. 5D). Clinical sample analysis revealed higher PA levels in steatotic HCC compared to nonsteatotic HCC, with a significant negative correlation between ADH1C expression and PA levels in steatotic HCC (Fig. 5E–F). Global palmitoylation and TEAD1 palmitoylation levels were higher in steatotic HCC than in nonsteatotic HCC, opposite to ADH1C expression patterns (Fig. 5G–I). We hypothesized that ADH1C-mediated reduction in PA concentration inhibits TEAD1 palmitoylation and TEAD1-YAP complex formation. This was validated by confirming TEAD1 auto-palmitoylation in HCC cells and showing that ADH1C negatively regulated TEAD1 palmitoylation (Fig. 5J–K). Exogenous PA supplementation rescued the reduced TEAD1-YAP binding caused by ADH1C overexpression, while the TEAD1 palmitoylation inhibitor VT103 reversed the increased binding due to ADH1C knockdown (Fig. 5L). Similarly, PA supplementation or VT103 reversed ADH1C-mediated changes in cell proliferation, cell cycle, and apoptosis (Figs. 5M, S11A–E). In a myr-AKT/NRAS12D-induced liver cancer model, dietary PA supplementation reversed the effects of ADH1C overexpression on tumor number and size, promoted vacuolar degeneration and lipid accumulation, and enhanced HCC proliferation (Fig. 5N–S). These findings indicate that ADH1C regulates PA concentration to inhibit TEAD1 palmitoylation and TEAD1-YAP complex formation.

2.9. ADH1C/PPARa axis regulates palmitic acid homeostasis and activation of Hippo pathway in HCC

Fatty acid oxidation is the sole degradation pathway for palmitic acid [30]. We investigated whether palmitic acid levels in HCC and TEAD1 palmitoylation are regulated by the ADH1C/PPARa axis. Results showed that PPARa knockdown reversed the inhibitory effect of ADH1C on palmitic acid levels in HCC cells (Fig. 6A) and reduced TEAD1 palmitoylation, thereby eliminating the effects of ADH1C overexpression (Fig. 6B). Additionally, PPARa knockdown abolished the effects of ADH1C overexpression on cell cycle progression and apoptosis (Figs. 6C–F, S11F–G). In an orthotopic steatotic liver cancer model (Fig. S2), PPARa knockdown rescued the decrease in palmitic acid content and TEAD1 palmitoylation levels in tumor tissues caused by ADH1C overexpression (Fig. 6G, H). Furthermore, changes in Hippo pathway target genes induced by ADH1C overexpression were restored by PPARa knockdown (Fig. 6I).

2.10. The co-expression of both ADH1C and PPARa can differentiate HCC subtypes and improve PD-1 efficacy

We evaluated the potential of the ADH1C/PPARa axis to assist clinical decision-making in HCC treatment. In both the steatotic HCC cohort from Zhongnan Hospital of Wuhan University and the TCGA-LIHC cohort, patients with high expression of both ADH1C and PPARa had significantly better survival compared to those with low expression of both genes. Patients with high expression of ADH1C or PPARa alone had intermediate survival rates (Figs. 7A, S12A). This suggests that ADH1C and PPARa could serve as joint prognostic factors in both steatotic and nonsteatotic HCC. Additionally, ADH1C and PPARa were significantly co-expressed in HCC tissues, with nonsteatotic HCC showing low expression and steatotic HCC showing high expression of both genes (Fig. 7B). This indicates their potential as biomarkers to differentiate between nonsteatotic and steatotic HCC. Accordingly, we developed a nomogram based on ADH1C and PPARa expression levels to diagnose steatotic HCC and guide clinical decisions (Fig. 7C). The Hosmer-Lemeshow test confirmed the nomogram's diagnostic value ($P > 0.05$), which was further visualized using a calibration curve

(Fig. 7D). Decision Curve Analysis demonstrated superior diagnostic performance of the nomogram compared to models using ADH1C or PPARa alone (Fig. 7E). A clinical impact curve also validated the model's effectiveness (Fig. 7F).

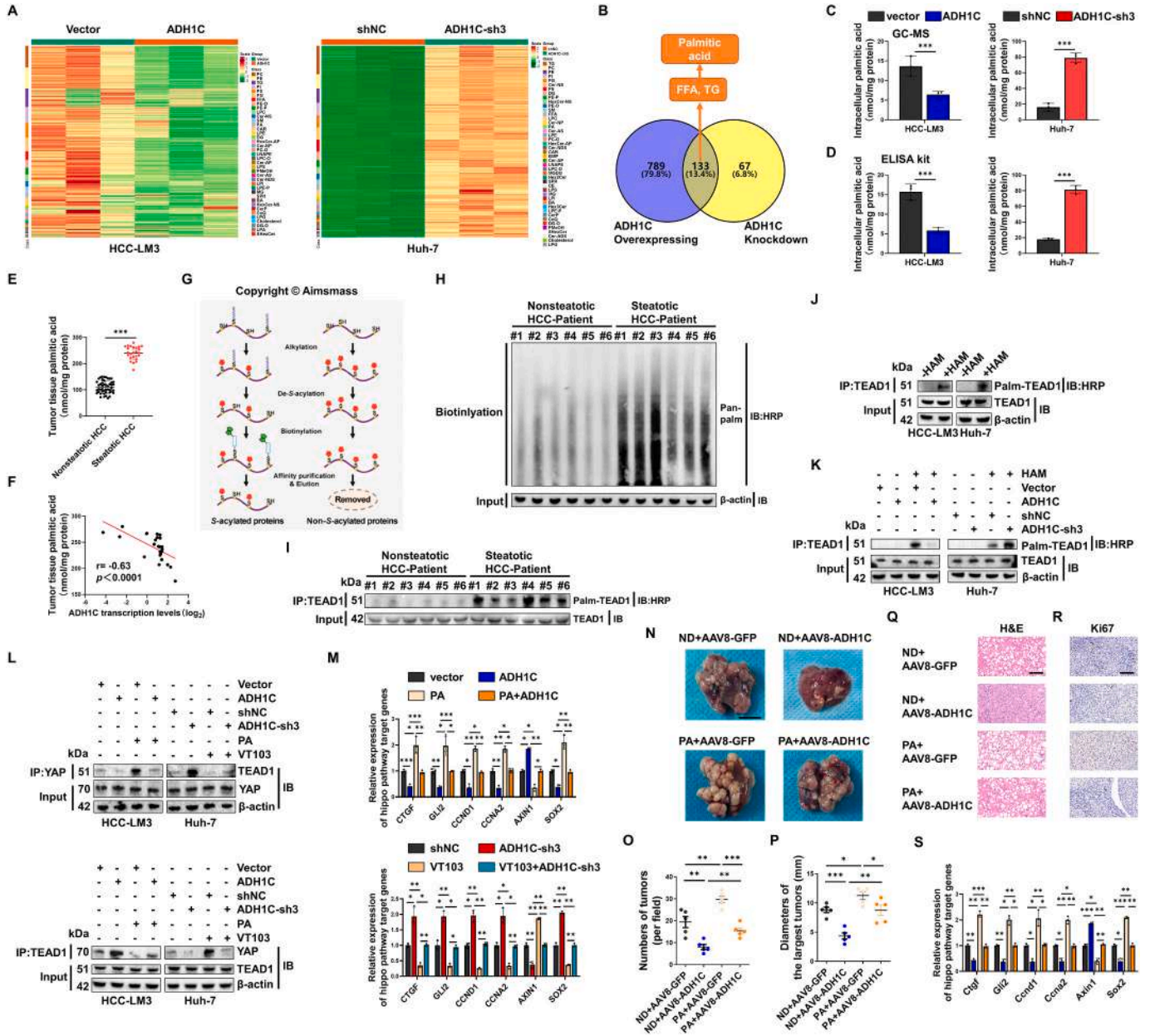
These findings suggest a potential synergistic effect of ADH1C and PPARa in HCC. To test this hypothesis, we overexpressed both ADH1C and PPARa in a myr-Akt/NRAS12D-induced mouse model of liver cancer (Fig. 7G). Overexpression of either ADH1C or PPARa alone reduced tumor number and the diameter of the largest tumor (Figs. 7H–I, S12E). Importantly, combined overexpression of ADH1C and PPARa further enhanced this inhibitory effect (Fig. 7H–I).

The study by Mathias Heikenwalder et al. showed that severe hepatic steatosis leads to inflammation and liver damage, impairing the efficacy of PD-1 immunotherapy despite higher PD-1 expression in steatotic HCC compared to nonsteatotic HCC [4]. We hypothesize that elevated palmitic acid levels contribute to this phenomenon, as palmitic acid induces immune exhaustion, inflammation, and liver damage [2,31]. Co-overexpression of ADH1C and PPARa reduced palmitic acid content in mouse HCC (Fig. 7J), while high intratumoral palmitic acid was observed in steatotic HCC patients with low ADH1C/PPARa expression (Fig. 7K). Consistent with previous reports [4], myr-AKT/NRAS12D-induced steatotic liver cancer exhibited higher PD-1 expression (Fig. S12F) and was unresponsive to anti-PD1 therapy (Fig. S12G–J). Conversely, nonsteatotic liver cancer induced by myr-Myc/NRAS12D responded to anti-PD1 treatment, with reduced tumor burden and prolonged survival (Fig. S12K–N). Exogenous palmitic acid supplementation in nonsteatotic liver cancer models also inhibited anti-PD1 efficacy (Fig. S12K–N). To investigate whether ADH1C could enhance anti-PD1 therapy in steatotic HCC, we treated myr-AKT/NRAS12D-induced steatotic liver cancer mice with AAV8-ADH1C and anti-PD1 (Fig. 7L). Results showed that while anti-PD1 alone was ineffective, AAV8-ADH1C significantly improved anti-PD1 efficacy (Fig. 7M). Combined treatment with AAV8-ADH1C and anti-PD1 maximally enhanced therapeutic outcomes, reducing tumor burden and significantly improving survival rates (Fig. 7N–P). In summary, ADH1C/PPARa expression is associated with lipid metabolism and serves as a prognostic factor in HCC. Targeting fatty acid catabolism may be an effective strategy for treating steatotic HCC and overcoming immunotherapy challenges.

3. Discussion

With the increasing prevalence of non-viral HCC due to antiviral therapy and dietary changes, steatotic HCC has emerged as an important subtype characterized by intracellular fat accumulation, vacuolar degeneration, and potential inflammatory infiltration and fibrosis [32,33]. Our analysis revealed that steatotic HCC often exhibits significant proliferative capacity and is associated with a unique metabolic microenvironment that reduces the efficacy of immunotherapy, highlighting the need for accurate patient stratification [4]. We identified ADH1C and PPARa as combined biomarkers to differentiate steatotic from non-steatotic HCC. Using a myr-Akt/NRAS12D-induced steatotic liver cancer model, we demonstrated that ADH1C+anti-PD1 therapy significantly enhanced treatment efficacy and survival, likely through reducing intratumoral palmitic acid content. Although the specific mechanisms remain to be elucidated, our findings suggest that ADH1C and low palmitic acid content are clinically relevant in HCC, as dietary palmitic acid supplementation can negate anti-PD1 efficacy in non-steatotic HCC models [5,34]. Further investigation into the pathways linking palmitic acid and anti-PD1 efficacy is warranted in the future.

PA constitutes 20-30% of total body fatty acids and can be obtained through diet or synthesized/degraded via fatty acid metabolism [5,30,34]. PA is a key metabolite in fatty acid metabolism, associated with tumor progression, including in steatotic HCC [35,36], and can induce immune exhaustion in this context [2]. However, current research mainly focuses on the tumor effects resulting from exogenous PA [34], neglecting the impact of PA degradation. Our study highlights



(caption on next page)

Fig. 5. ADH1C inhibits the palmitoylation level of TEAD1 by reducing intracellular palmitic acid levels.

A GC–MS lipidomics analysis was conducted on cells with ADH1C overexpression or knockdown.

B Venn diagrams displayed the shared differential metabolites in the ADH1C overexpression and knockdown groups.

C Palmitic acid content in HCC cells was quantified using GC–MS.

D Palmitic acid content in HCC cells was measured via enzyme-linked reaction (ELISA) method.

E ELISA method was used to measure palmitic acid content in steatotic HCC and nonsteatotic HCC tissues.

F Pearson analysis revealed the correlation between ADH1C mRNA levels and palmitic acid content in steatotic HCC.

G Schematic illustration of the Acyl-biotin Exchange (ABE) method for detecting protein palmitoylation modification.

H ABE method was employed to capture palmitoylated proteins in steatotic HCC and nonsteatotic HCC tissues, followed by protein immunoblot analysis to quantify the presence of palmitoylated proteins in the tissues. HAM: hydroxylamine.

I ABE method was used to capture palmitoylated TEAD1 in steatotic HCC and nonsteatotic HCC tissues, followed by protein immunoblot analysis to quantify the level of palmitoylated TEAD1.

J ABE method and protein immunoblot were used to detect the auto-palmitoylation level of TEAD1 in HCC cells. HAM: hydroxylamine.

K ABE method and protein immunoblot were used to detect the palmitoylation level of TEAD1 in cells with ADH1C overexpression or knockdown. HAM: hydroxylamine.

L–M HCC cells with ADH1C overexpression or knockdown were treated with palmitic acid (1 mM) for 24 h or TEAD1 palmitoylation inhibitor VT103 (3 μ M) for 4 h.

COIP was used to assess the binding capacity of YAP–TEAD1 (L), and qRT-PCR was used to detect mRNA levels of Hippo signaling pathway target genes (M).

N Livers from myr-Akt/NRas12D infected mice with or without ADH1C overexpression, and with or without a high-palmitic acid diet. Scale bars, 10 mm.

O–P Numbers of tumors (per field) (O), Diameters of the largest tumors (P) in livers from myr-Akt/NRas12D infected mice with or without ADH1C overexpression, and with or without a high-palmitic acid diet.

Q–R HE (Q), and Ki67 staining (R) in livers from myr-Akt/NRas12D infected mice with or without ADH1C overexpression, and with or without a high-palmitic acid diet. Scale bars, 100 μ m.

S qRT-PCR was used to detect mRNA levels of Hippo signaling pathway target genes in livers from myr-Akt/NRas12D infected mice with or without ADH1C overexpression, and with or without a high-palmitic acid diet. Scale bars, 100 μ m.

* ($p < 0.05$), ** ($p < 0.01$), or *** ($p < 0.001$).

the crucial role of fatty acid degradation in steatotic HCC, with ADH1C as a key regulator. Reduced ADH1C expression impairs fatty acid oxidation, elevating endogenous PA levels in HCC. PA exhibits unique functions compared to other saturated fatty acids, binding to specific cysteine residues in target proteins to form reversible thioester bonds, thereby regulating protein localization, stability, and interactions, and impacting cellular signaling pathways [29,30,34,37,38]. We found that ADH1C-mediated regulation of intracellular PA levels dynamically modulates the palmitoylation of TEAD1, a key Hippo pathway transcription factor, and its interaction with YAP, thereby affecting HCC cell proliferation. Since ADH1C influences intracellular PA levels, it likely regulates palmitoylation of other key proteins. Future research will explore whether other features of steatotic HCC, such as inflammation and fibrosis, are also regulated by palmitoylation.

We also elucidate a novel mechanism by which ADH1C inhibits fatty acid metabolism reprogramming in HCC. ADH1C promotes fatty acid β -oxidation by regulating the expression of the fatty acid oxidation-related transcription factor PPAR α and upregulating key fatty acid oxidation enzymes, such as CPT1a and ACOX1. Mechanistically, ADH1C enhances PPAR α mRNA and protein expression by promoting the pre-mRNA splicing of PPAR α CDS. Alternative splicing is crucial in aberrant fatty acid metabolism in cancer cells, where disrupted splicing processes and tumor-associated splice variants can alter gene expression patterns and contribute to HCC development [39,40]. While PPAR α is known to undergo aberrant pre-mRNA splicing in nonalcoholic fatty liver disease (NAFLD) [17], its role in HCC has not been reported. Our study shows that ADH1C regulates PPAR α CDS pre-mRNA splicing by interacting with RP9, which promotes RP9 binding to PPAR α exon 8, enhances pre-mRNA splicing of PPAR α exons 8–9, and upregulates mature PPAR α mRNA, thereby increasing fatty acid catabolism. Downregulation of wild-type PPAR α mediates the effects of ADH1C downregulation in HCC. Furthermore, we elucidated the specific molecular mechanisms underlying ADH1C/RP9-mediated regulation of PPAR α alternative splicing through in vitro experiments. ADH1C competes with PPP1CA for RP9 binding, preventing RP9 dephosphorylation. The phosphorylated RP9 localizes to nuclear speckles, where it promotes PPAR α pre-mRNA splicing. The altered splicing activity of RP9 mediated by ADH1C likely affects the splicing patterns of other genes, which requires further investigation.

In summary, our study confirmed that ADH1C downregulation promotes HCC by reshaping fatty acid metabolism toward lipid

accumulation (particularly palmitic acid) via alternative splicing of PPAR α , as demonstrated through multi-omics analysis. We also established that ADH1C and PPAR α , as combined biomarkers, can effectively distinguish fatty and non-fatty HCC, providing a new tool for precise diagnosis and stratified treatment. The proposed metabolic treatment strategy targeting the ADH1C/PPAR α axis may transform HCC treatment and is anticipated to be verified in clinical trials. Additionally, the diagnostic model based on ADH1C and PPAR α could be developed into non-invasive clinical tools, such as liquid biopsy markers or imaging targets, for early detection and monitoring of HCC.

However, limitations remain. While we elucidated the role of the ADH1C-RP9-PPAR α axis in fatty acid oxidation, the broader impact of ADH1C on pre-mRNA splicing patterns through RP9 remains unconfirmed. Furthermore, although ADH1C is downregulated in both steatotic and non-steatotic HCC compared to non-tumor tissues, its role in non-steatotic HCC, where PA-induced palmitoylation of TEAD1 may not be as prominent, requires further investigation.

4. Methods

The following is a brief description of the **KEY methods**. All more detailed methodologies can be found in Supplementary Materials and Methods.

4.1. Collection of HCC tissue sample

Tissues: Proteomics analysis was performed on 3 steatotic and 3 nonsteatotic HCC tissues from patients without alcohol/viral/chemotherapy history. An additional 72 paired HCC/non-tumor tissues (25 steatotic, 47 nonsteatotic) were collected from Zhongnan Hospital. Diagnoses were confirmed by two pathologists. Ethical approval (KELUN, 2018010) and informed consent were obtained.

4.2. Mouse models & in vivo experiments

Tumor induction: Hepatic tumors in C57BL/6J mice were generated via hydrodynamic tail vein injection (HTVi) of oncogenic plasmids (Akt, NRasV12, SB transposase).

Gene modulation: Hepatocyte-specific AAV8 vectors (Alb promoter) delivered ADH1C/PPAR α .

Treatments:

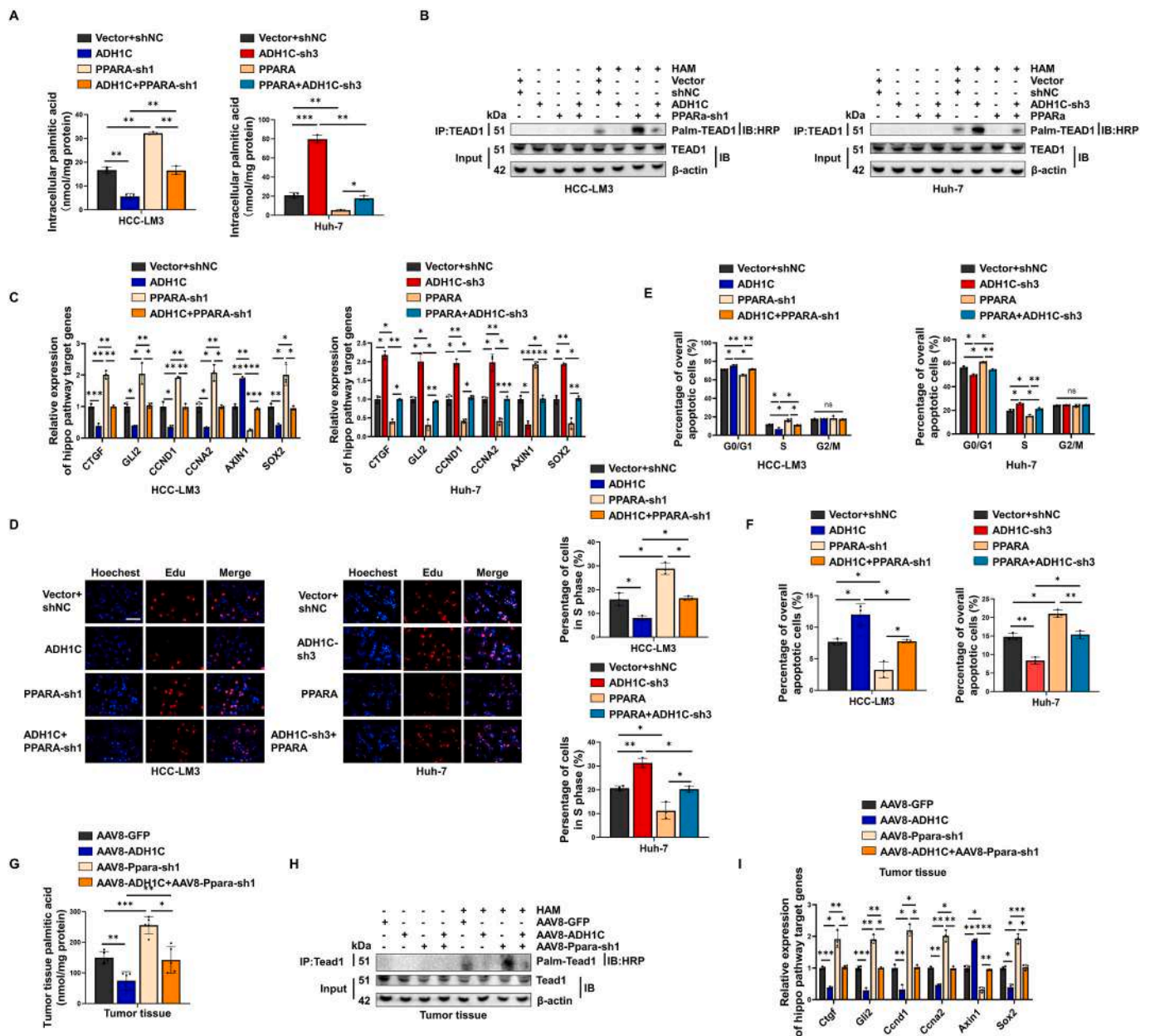


Fig. 6. ADH1C regulates palmitic acid content and palmitoylation of TEAD1 in HCC cells through PPARα. A–F In HCC cells with ADH1C overexpression or knockdown, PPARα was either knocked down or overexpressed. The Enzyme-linked Immunosorbent Assay (ELISA) method was used to detect the palmitic acid (PA) content in HCC cells (A). The Acyl-biotin Exchange (ABE) method and protein immunoblot analysis were utilized to assess the palmitoylation level of TEAD1 in HCC cells (B). qRT-PCR was used to measure the mRNA levels of Hippo signaling pathway target genes in HCC cells (C). EDU staining was used to label HCC cells in the S phase (D). Flow cytometry was utilized to screen HCC cells in different cell cycle phases and calculate their proportions (E). Flow cytometry was used to screen HCC cells in various apoptosis stages and calculate their proportions (F). HAM: hydroxylamine. G–I In the myr-Akt/NRas12D-induced steatotic liver cancer mouse model with ADH1C overexpression, high-pressure hydrodynamic was used to knock down PPARα in the mouse liver. ELISA was used to measure the palmitic acid content in liver tumors (G). ABE method and protein immunoblot analysis were used to assess the palmitoylation level of TEAD1 in liver tumors (H). qRT-PCR was used to measure the mRNA levels of Hippo signaling pathway target genes in HCC cells (I). HAM: hydroxylamine.

* (p < 0.05), ** (p < 0.01), or *** (p < 0.001).

Palmitate (PA, 10 mg/kg, i.p.) to modulate metabolism.
 Anti-PD-1 (300 μg, i.p., every 5 days) to assess immunotherapy synergy.
 Ethics: Approved by Wuhan University's IACUC (No. ZN2022178).

4.3. Multi-omics & bioinformatics

Transcriptomics: RNA-seq (Illumina NovaSeq) after Agilent 2100 quality control.

Lipidomics: LC-MS/MS analysis of lipid extracts (methanol/MTBE extraction).
 Proteomics: iTRAQ/TMT-labeled peptides analyzed by LC-MS/MS (Q Exactive). Database searches used MASCOT (FDR ≤ 0.01).
 TCGA data: Analyzed 374 HCC samples for differential expression (|log2FC| > 1, adj. p < 0.05) and pathways (GSEA/KEGG).

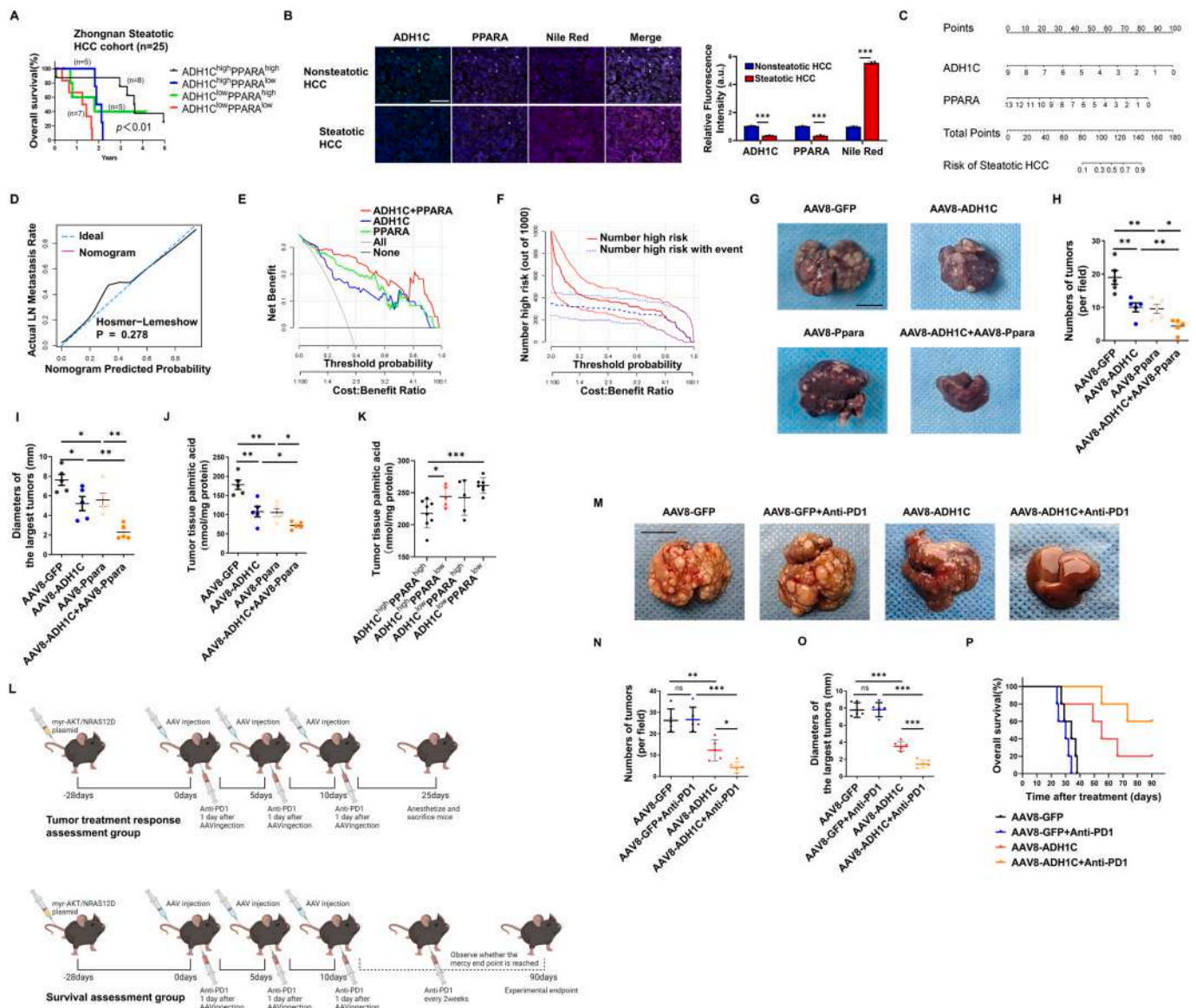


Fig. 7. Co-expression of ADH1C and PPARα can jointly diagnose and differentiate steatotic HCC and improve the efficacy of anti-PD-1. A Survival curve analysis of steatotic HCC patients based on ADH1C and PPARα expression in the Zhongnan Hospital of Wuhan University cohort. B Immunofluorescence analysis showing the co-expression of ADH1C and PPARα, as well as the neutral lipid content, in steatotic HCC and nonsteatotic HCC patients. Scale bars, 100 μm. C Construction of a diagnostic model for steatotic HCC based on ADH1C and PPARα mRNA expression using a column plot. D Hosmer-Lemeshow goodness-of-fit test assessing the diagnostic value of the column plot, further visualized using a calibration curve. E Decision curve analysis (DCA) curve demonstrating the performance of the combined ADH1C+PPARα diagnostic model for steatotic HCC compared to diagnostic models based on ADH1C or PPARα alone. F Clinical impact curve displaying the diagnostic performance of the combined ADH1C+PPARα diagnostic model for steatotic HCC. G-J In the myr-Akt/NRas12D-induced steatotic liver cancer mouse model with individual or co-overexpression of ADH1C and PPARα. Livers from the mentioned model. Scale bars, 10 mm (G). Number of tumors per field (H), diameters of the largest tumors (I) in livers from the mentioned model. The Enzyme-linked Immunosorbent Assay (ELISA) method was used to detect the palmitic acid (PA) content in liver tumors (J). K ELISA-based analysis of PA content in steatotic HCC based on ADH1C and PPARα mRNA levels. L-P Combination therapy using AAV8-ADH1C, AAV8-PPARα, and anti-PD-1 in the myr-Akt/NRas12D-induced steatotic liver cancer mouse model. Illustration of the mentioned model (L). Gross appearance of the liver in the mentioned model. Scale bars, 10 mm (M). Number of tumors per field (N), diameters of the largest tumors (O) in the mentioned model. Survival curve of the mentioned model mice (P). * (p < 0.05), ** (p < 0.01), or *** (p < 0.001).

4.4. Molecular biology

Cell culture: HCC lines (Huh-7, Hep3B, etc.) and normal hepatocytes (MIHA) cultured in DMEM/MEM + 10 % FBS, validated by STR profiling.

Gene manipulation: siRNA/shRNA (Qingke Biotech), plasmids (Jet-PRIME®), and AAVs for overexpression/knockdown.

Assays:

qRT-PCR/WB: RNA/protein extraction (Easyspin/RIPA kits), SYBR

Green qPCR, and ECL detection.

Co-IP/RIP: Protein-protein/RNA interactions analyzed by MS/WB.

Proliferation: Colony formation and EdU assays.

Palmitoylation: ABE kits for TEAD1 modification detection.

4.5. Metabolic analyses

Enzyme activity: ADH1C measured (Macklin kit).

Lipid content: Triglycerides, cholesterol, free fatty acids (Nanjing

Jiancheng kits).

FAO: Oxygen consumption (Abcam kit) with oleate/FCCP.

Palmitate: ELISA (Mlbio).

Visualization: Nile Red staining for lipid droplets.

4.6. Pathological techniques

IHC/IF: Antigen retrieval, DAB staining (IHC), and DAPI/antibody labeling (IF; OLYMPUS confocal).

Phospho-antibodies: Custom-generated via peptide immunization (RP9 S169).

4.7. Statistics

Tools: SPSS 25.0, GraphPad Prism 8.0.

Tests: Shapiro-Wilk (normality), *t*-tests/Wilcoxon (two groups), ANOVA (multi-group), Kaplan-Meier (survival), Pearson (correlations).

Significance: $p < 0.05$, $*p < 0.01$, $**p < 0.001$.

Supplementary data to this article can be found online at <https://doi.org/10.1016/j.metabol.2025.156267>.

Abbreviations

HCC	Hepatocellular carcinoma
ADH1C	Alcohol dehydrogenase 1C
RP9	Retinitis pigmentosa 9
PPARα	Peroxisome proliferator activated receptor alpha
TEAD1	TEA domain transcription factor 1
PD1	Programmed cell death protein 1
ICIs	Immune checkpoint inhibitors
CTLA-4	Cytotoxic T-lymphocyte associated protein 4
PD-L1	Programmed cell death ligand 1
HBV	Hepatitis B virus
AKT	AKT serine/threonine kinase 1
ADH	Alcohol dehydrogenase
YAP	Yes1 associated transcriptional regulator
PMSF	Phenylmethylsulfonyl fluoride
EDTA	Ethylene diamine tetraacetic acid
MTBE	Methyltert-butylether
LC-MS	Liquid chromatograph-mass spectrometry
MS	Mass spectrometry
TCGA	The Cancer Genome Atlas
KEGG	Kyoto Encyclopedia of Genes and Genomes
GSEA	Gene Set Enrichment Analysis
URLs	Universal Resource Locators
DMEM	Dulbecco's Modified Eagle's medium
FBS	Fetal bovine serum
MEM	Minimal essential medium
PCR	Polymerase Chain Reaction
qRT-PCR	RNA extraction, real-time quantitative PCR
WB	Western blot analysis
RIPA	Radio-Immunoprecipitation Assay
PVDF	Polyvinylidene difluoride
ECL	Electrochemiluminescence
EdU	5-ethynyl-2'-deoxyuridine
HTVi	Tail vein hydrodynamic injection
SPSS	Statistical Product and Service Solutions
CDS	Coding sequence
ND	Normal diet
IACUC	Institutional Animal Care and Use Committee
IHC	Immunohistochemistry
IF	Immunofluorescence
BSA	Blocking buffer
DAB	3,3'-Diaminobenzidine
PBS	Phosphate-buffered saline
NP-40	Nonidet P-40

DAPI	4',6-diamidino-2-phenylindole
co-IP	Coimmunoprecipitation
SDS	Sodium dodecyl sulfate
RIP	RNA immunoprecipitation
FAO	Fatty acid oxidation
FCCP	Carbonyl cyanide 4-(trifluoromethoxy)phenylhydrazone
GO	Gene Ontology
TG	Triglyceride
FFA	Free fatty acid
CTGF	Cellular communication network factor 2
GLI2	GLI family zinc finger 2
CCND1	Cyclin D1
CCNA2	Cyclin A2
SOX2	SRY-box transcription factor 2
AXIN1	Axin 1
Gal4	Galactose-responsive transcription factor GAL4
PI	Phosphatidyl inositol
PC	Phosphatidyl cholines
CPT1a	Carnitine palmitoyltransferase 1A
CPT2	Carnitine palmitoyltransferase 2
ACOX	Acyl-CoA oxidase 1
CACT	Solute carrier family 25 member 20
EX	Exon
PPP1CA	Protein phosphatase 1 catalytic subunit alpha
DCA	Decision Curve Analysis
PA	Palmitic acid
NAFLD	Nonalcoholic fatty liver disease

CRedit authorship contribution statement

Kequan Xu: Writing – review & editing, Writing – original draft, Visualization, Validation, Methodology, Formal analysis, Data curation, Conceptualization. **Tianguen Wu:** Writing – original draft, Validation, Supervision, Resources, Formal analysis, Data curation. **Xiaomian Li:** Writing – original draft, Methodology, Formal analysis, Data curation. **Xiao Zhang:** Writing – original draft, Visualization, Validation, Formal analysis, Data curation. **Xinyu Liu:** Visualization, Methodology. **Shuxian Ma:** Validation. **Wenlong Dong:** Methodology. **Jialing Yang:** Data curation. **Yingyi Liu:** Resources. **Weixian Fang:** Methodology. **Yi Ju:** Methodology. **Yiran Chen:** Software. **Caixia Dai:** Software. **Zheng Gong:** Validation. **Wenzhi He:** Methodology. **Zan Huang:** Investigation. **Lei Chang:** Resources. **Weijie Ma:** Resources. **Peng Xia:** Writing – review & editing, Writing – original draft, Resources, Investigation, Formal analysis, Conceptualization. **Xi Chen:** Writing – review & editing, Writing – original draft, Visualization, Resources, Funding acquisition, Data curation, Conceptualization. **Yufeng Yuan:** Writing – review & editing, Writing – original draft, Supervision, Software, Resources, Project administration, Investigation, Funding acquisition, Conceptualization.

Ethics statement

The study was approved by the Hospital's Protection of Human Subjects Committee (KELUN, 2018010). All animal experiments were conducted in strict accordance with the Guide for the Care and Use of Laboratory Animals and approved by the Laboratory Animal Ethics Committee (ZN2022178), Zhongnan Hospital of Wuhan University (Hubei Province, China).

Funding statement

This work was supported by the National Natural Science Foundation of China (824B2088); National Natural Science Foundation of China (82300675); Research Fund of the Health Commission of Hubei Province (WJ2021M255); Cancer Research and Translational Platform Project of Zhongnan Hospital of Wuhan University (ZLYNXM202004);

Key Research and Development Program of Hubei Province (2021BCA114); the Research Fund from the Medical Sci-Tech Innovation Platform of Zhongnan Hospital of Wuhan University (PTXM2021022); the China National Postdoctoral Program for Innovative Talents (BX20240271); the China Postdoctoral Science Foundation (2023M742698); the National Natural Science Foundation of China (82403904); the Natural Science Foundation of Hubei Province (2024AFB163); the Fundamental Research Funds for the Central Universities (413000553).

Declaration of competing interest

The authors declare that they have no competing interests.

Acknowledgements

We acknowledge and appreciate all of our colleagues at the Medical Research Center for their valuable suggestions and technical assistance.

Data availability

Generated bulk RNA-seq data have been deposited at GEO (GSE273402 and GSE273403). Additionally, this paper utilizes existing, publicly available data. Accession numbers for the datasets are listed in the key resources table and in associated figure legends. Flow cytometry, microscopy, and western blot data are available upon request.

References

- Toh MR, Wong EYT, Wong SH, Ng AWT, Loo LH, Chow PK, et al. Global epidemiology and genetics of hepatocellular carcinoma. *Gastroenterology* 2023; 164(5):766–82.
- Murai H, Kodama T, Maesaka K, Tange S, Motooka D, Suzuki Y, et al. Multiomics identifies the link between intratumor steatosis and the exhausted tumor immune microenvironment in hepatocellular carcinoma. *Hepatology* 2023;77(1):77–91.
- Foglia B, Beltra M, Sutti S, Cannito S. Metabolic reprogramming of HCC: a new microenvironment for immune responses. *Int J Mol Sci* 2023;24(8).
- Pfister D, Nunez NG, Pinyol R, Govaere O, Pinter M, Szydlowska M, et al. NASH limits anti-tumour surveillance in immunotherapy-treated HCC. *Nature* 2021;592(7854):450–6.
- Xu K, Xia P, Chen X, Ma W, Yuan Y. ncRNA-mediated fatty acid metabolism reprogramming in HCC. *Trends Endocrinol Metab* 2023;34(5):278–91.
- Canestro C, Godoy L, Gonzalez-Duarte R, Albalat R. Comparative expression analysis of Adh3 during arthropod, urochordate, cephalochordate, and vertebrate development challenges its predicted housekeeping role. *Evol Dev* 2003;5(2): 157–62.
- Edenberg HJ. The genetics of alcohol metabolism: role of alcohol dehydrogenase and aldehyde dehydrogenase variants. *Alcohol Res Health* 2007;30(1):5–13.
- Li S, Yang H, Li W, Liu JY, Ren LW, Yang YH, et al. ADH1C inhibits progression of colorectal cancer through the ADH1C/PHGDH/PSAT1/serine metabolic pathway. *Acta Pharmacol Sin* 2022;43(10):2709–22.
- Su JS, Tsai TF, Chang HM, Chao KM, Su TS, Tsai SF. Distant HNF1 site as a master control for the human class I alcohol dehydrogenase gene expression. *J Biol Chem* 2006;281(29):19809–21.
- Oota H, Dunn CW, Speed WC, Pakstis AJ, Palmatier MA, Kidd JR, et al. Conservative evolution in duplicated genes of the primate class I ADH cluster. *Gene* 2007;392(1–2):64–76.
- Hatano M, Ojima H, Masugi Y, Tsujikawa H, Hiraoka N, Kanai Y, et al. Steatotic and nonsteatotic scirrhous hepatocellular carcinomas reveal distinct clinicopathological features. *Hum Pathol* 2019;86:222–32.
- Mohamad B, Shah V, Onyshchenko M, Elshamy M, Aucejo F, Lopez R, et al. Characterization of hepatocellular carcinoma (HCC) in non-alcoholic fatty liver disease (NAFLD) patients without cirrhosis. *Hepatol Int* 2016;10(4):632–9.
- Kampe K, Sieber J, Orellana JM, Mundel P, Jehle AW. Susceptibility of podocytes to palmitic acid is regulated by fatty acid oxidation and inversely depends on acetyl-CoA carboxylases 1 and 2. *Am J Physiol Renal Physiol* 2014;306(4):F401–9.
- Ameer F, Scanduzzi L, Hasnain S, Kalbacher H, Zaidi N. De novo lipogenesis in health and disease. *Metabolism* 2014;63(7):895–902.
- Yang T, Liang N, Zhang J, Bai Y, Li Y, Zhao Z, et al. OCTN2 enhances PGC-1alpha-mediated fatty acid oxidation and OXPHOS to support stemness in hepatocellular carcinoma. *Metabolism* 2023;147:155628.
- Fujiwara N, Nakagawa H, Enooku K, Kudo Y, Hayata Y, Nakatsuka T, et al. CPT2 downregulation adapts HCC to lipid-rich environment and promotes carcinogenesis via acylcarnitine accumulation in obesity. *Gut* 2018;67(8): 1493–504.
- Jobbins AM, Haberman N, Artigas N, Amourda C, Paterson HAB, Yu S, et al. Dysregulated RNA polyadenylation contributes to metabolic impairment in non-alcoholic fatty liver disease. *Nucleic Acids Res* 2022;50(6):3379–93.
- Antwi MB, Lefere S, Clarisse D, Koorneef L, Heldens A, Onghena L, et al. PPARalpha-ERRalpha crosstalk mitigates metabolic dysfunction-associated steatotic liver disease progression. *Metabolism* 2025;164:156128.
- Takeyama K, Kodera Y, Suzawa M, Kato S. Peroxisome proliferator-activated receptor (PPAR)—structure, function, tissue distribution, gene expression. *Nihon Rinsho* 2000;58(2):357–63.
- Schoonjans K, Staels B, Auwerx J. The peroxisome proliferator activated receptors (PPARs) and their effects on lipid metabolism and adipocyte differentiation. *Biochim Biophys Acta* 1996;1302(2):93–109.
- Maita H, Kitaura H, Keen TJ, Inglehearn CF, Ariga H, Iguchi-Ariga SM. PAP-1, the mutated gene underlying the RP9 form of dominant retinitis pigmentosa, is a splicing factor. *Exp Cell Res* 2004;300(2):283–96.
- Sharma K, D'Souza RC, Tyanova S, Schaab C, Wisniewski JR, Cox J, et al. Ultra-deep human phosphoproteome reveals a distinct regulatory nature of Tyr and Ser/Thr-based signaling. *Cell Rep* 2014;8(5):1583–94.
- Zhang B, Xie SH, Hu JY, Lei SJ, Shen LH, Liu HT, et al. Truncated SCRIB isoform promotes breast cancer metastasis through HNRNP A1 mediated exon 16 skipping. *Acta Pharmacol Sin* 2023;44(11):2307–21.
- Yadav SP, Hao H, Yang HJ, Kautzmann MA, Brooks M, Nellisery J, et al. The transcription-splicing protein NonO/p54nrb and three NonO-interacting proteins bind to distal enhancer region and augment rhodopsin expression. *Hum Mol Genet* 2014;23(8):2132–44.
- Khan MM, Valikangas T, Khan MH, Moulder R, Ullah U, Bhosale SD, et al. Protein interactome of the cancerous inhibitor of protein phosphatase 2A (CIP2A) in Th17 cells. *Curr Res Immunol* 2020;1:10–22.
- Dey A, Varelas X, Guan KL. Targeting the hippo pathway in cancer, fibrosis, wound healing and regenerative medicine. *Nat Rev Drug Discov* 2020;19(7):480–94.
- Zheng Y, Pan D. The hippo signaling pathway in development and disease. *Dev Cell* 2019;50(3):264–82.
- Zanconato F, Forcato M, Battilana G, Azzolin L, Quaranta E, Bodega B, et al. Genome-wide association between YAP/TAZ/TEAD and AP-1 at enhancers drives oncogenic growth. *Nat Cell Biol* 2015;17(9):1218–27.
- Chan P, Han X, Zheng B, DeRan M, Yu J, Jarugumilli GK, et al. Autopalmitoylation of TEAD proteins regulates transcriptional output of the hippo pathway. *Nat Chem Biol* 2016;12(4):282–9.
- Carta G, Murru E, Banni S, Manca C. Palmitic acid: physiological role. *Metabolism and Nutritional Implications Front Physiol* 2017;8:902.
- Ren Q, Sun Q, Fu J. Dysfunction of autophagy in high-fat diet-induced non-alcoholic fatty liver disease. *Autophagy* 2024;20(2):221–41.
- Llovet JM, Kelley RK, Villanueva A, Singal AG, Pikarsky E, Roayaie S, et al. Hepatocellular carcinoma. *Nat Rev Dis Primers* 2021;7(1):6.
- European Association for the Study of the Liver. Electronic address eee, European Association for the Study of the Liver. The EASL clinical practice guidelines: management of hepatocellular carcinoma. *J Hepatol* 2018;69(1):182–236.
- Bu L, Zhang Z, Chen J, Fan Y, Guo J, Su Y, et al. High-fat diet promotes liver tumorigenesis via palmitoylation and activation of AKT. *Gut* 2024;73(7):1156–68.
- Xu W, Zhang X, Wu JL, Fu L, Liu K, Liu D, et al. O-GlcNAc transferase promotes fatty liver-associated liver cancer through inducing palmitic acid and activating endoplasmic reticulum stress. *J Hepatol* 2017;67(2):310–20.
- Pascual G, Dominguez D, Elosua-Bayes M, Beckedorff F, Laudanna C, Bigas C, et al. Dietary palmitic acid promotes a prometastatic memory via Schwann cells. *Nature* 2021;599(7885):485–90.
- Kim NG, Gumbiner BM. Cell contact and Nf2/Merlin-dependent regulation of TEAD palmitoylation and activity. *Proc Natl Acad Sci U S A* 2019;116(20): 9877–82.
- Lv D, Cao X, Zhong L, Dong Y, Xu Z, Rong Y, et al. Targeting phenylpyruvate restrains excessive NLRP3 inflammasome activation and pathological inflammation in diabetic wound healing. *Cell Rep Med* 2023;4(8):101129.
- Berasain C, Elizalde M, Urtasun R, Castillo J, Garcia-Irigoyen O, Uriarte I, et al. Alterations in the expression and activity of pre-mRNA splicing factors in hepatocarcinogenesis. *Hepat Oncol* 2014;1(2):241–52.
- Zhou J, Chen W, He Q, Chen D, Li C, Jiang C, et al. SERBP1 affects the apoptotic level by regulating the expression and alternative splicing of cellular and metabolic process genes in HeLa cells. *PeerJ* 2022;10:e14084.